 CMES, vol.86, no.4, pp.275-300, 2012

A Localized RBF Meshfree Method for the Numerical Solution of the Kdv-Burger's Equation

G. C. Bourantas[1] **and V. C. Loukopoulos**[2]

Abstract: This paper formulates a local Radial Basis Functions (LRBFs) collocation method for the numerical solution of the non-linear dispersive and dissipative KdV-Burger's (KdVB) equation. This equation models physical problems, such as irrotational incompressible flow, considering a shallow layer of an inviscid fluid moving under the influence of gravity and the motion of solitary waves. The local type of approximations used, leads to sparse algebraic systems that can be solved efficiently. The Inverse Multiquadrics (IMQ), Gaussian (GA) and Multiquadrics (MQ) Radial Basis Functions (RBF) interpolation are employed for the construction of the shape functions. Accuracy of the method is assessed in terms of the L_2 and L_∞ error norms and three conservative properties related to mass, momentum and energy. Additionally we investigate how both the accuracy and the stability of the proposed method are affected from the number of nodes in the support domain, the parameter dependent RBFs, the condition number of the resulting algebraic systems and finally the time step length. Numerical experiments demonstrate the accuracy and the robustness of the method for solving nonlinear dispersive and dissipative problems, while stability analysis demonstrates that the numerical scheme is conditionally stable.

Keywords: Meshfree point collocation method; RBF; KdV-Burger; Solitons; Dissipative; Dispersive.

1 Introduction

The theoretical study of the irrotational incompressible flow, considering a shallow layer of an inviscid fluid moving under the influence of gravity, has attracted a great interest among the scientific community. Additionally, surface tension and particularly the motion of solitary waves has been an interesting subject of research

[1] Institute of Chemical Engineering and High Temperature Chemical Processes - Foundation for Research and Technology, P.O. Box 1414, GR-26504, Patras, Rion, Greece
[2] Department of Physics, University of Patras, Patras, 26500, Rion, Greece

for more than a century [Whitham 1974]. An interesting equation, initially formulated in [Su and Gardner (1969)], with numerous applications is the KdV-Burgers' equation. Kortewege-de Vries-Burgers' equation is a nonlinear partial differential equation, which is given by

$$\frac{\partial u}{\partial t}+\varepsilon u\frac{\partial u}{\partial x}-\nu\frac{\partial^2 u}{\partial x^2}+\mu\frac{\partial^3 u}{\partial x^3}=0, \tag{1}$$

where ε, ν and μ are positive parameters. In fact, the small parameters ε and μ are related to a small-amplitude and a long-wavelength assumption, respectively and, ν is the kinematic viscosity. Furthermore, the right-hand side of Eq. (1) is not actually zero in general, but is comprised of terms of order ε^2, μ^2 and $\varepsilon\mu$ which are neglected in the KdV-Burger approximation.

More precisely, this model arises in numerous physical applications such as propagation of waves in elastic tube filled with a viscous fluid [Jonson (1970)] and weakly non-linear plasma waves with certain dissipative effects [Grad and Hu (1967)]. It represents long wavelength approximations where effects of the non-linear advection term $u\frac{\partial u}{\partial x}$ are counterbalanced by the dispersion $\frac{\partial^3 u}{\partial x^3}$. Numerous theoretical issues related the KdV-Burger equation have received considerable attention, over the last years. Authors in [Demeiray (1998)] and [Antar and Demiray (1997)] derived KdVB equation as the governing evolution equation for wave propagation in fluid-filled elastic or viscoelastic tubes in which the effects of dispersion, dissipation and non-linearity were present. KdV-Burger equation can be regarded as the combination of the Burgers' equation (μ=0) and the KdV equation (ν=0). The former equation was first used by Burger in 1939 [Burger (1939)] for the study of turbulence (Burger's equation can be considered as linearized Navier-Stokes equations), while the later equation was first suggested by Kortewege and de Vries [Kortewege and de Vries (1895)], who studied the change in shape of long waves moving in a rectangular shallow water channel.

A considerable number of researchers solved the KdV-Burger equations using well-established numerical methods. In details, authors in [Zaki (2000)] have used quintic B-spline finite elements method. An algorithm, based on the collocation method with quintic B-spline finite elements, was set up in order to simulate the solutions of the KdV, Burgers' and the KdV-Burger equations, along with the migration of solitary waves and the temporal evolution of a Maxwellian initial pulse. Burgers' equation was also solved for different values of Reynolds number, while the time evaluation of the solutions of the KdVB equation with different values of the diffusion and dispersion coefficients was also examined. Invariants and error norms were studied for the determination of the conservation properties of the algorithm, while a linear stability analysis showed that the scheme was unconditionally stable.

Furthermore, in [Talaat and El-Danaf (2008)] authors used a septic B-spline and they obtained numerical methods for solution of KdVB equation. By applying the Von-Neumann stability analysis technique, the authors showed that the method is unconditionally stable. By conducting a comparison between the absolute error for the obtained numerical results and the analytic solution of the equation the accuracy of the proposed method was tested. In [Kaya and Aassila (2006), Soliman (2006)], authors utilized a decomposition method along with a variational iteration method in order to obtain exact solution of KdV-Burger equation. More precisely, in [Kaya and Aassila (2006)] the explicit solutions for the generalized Korteweg–de Vries equation with initial condition were calculated by using the Adomian Decomposition Method (ADM), indicating that the decomposition method is efficient and accurate, while in [Soliman (2006)] a variational iteration method for the solution of the Korteweg-de Vries Burgers (for short, KdVB) was obtained and the numerical results were compared with those calculated using an Adomian Decomposition Method. The comparison demonstrates that the two obtained solutions are in an excellent agreement. As the authors claim, the numerical results calculated show that the variational iteration method can be readily implemented to this type of nonlinear equations with excellent accuracy.

Over the past two decades a new class of numerical methods has emerged. Motivated, in part, by the difficulties that are present in the traditional numerical methods, such as FEM, FDM, FVM, BEM and Spectral [Liu (2002), Atluri and Shen (2002)], meshless (or meshfree) methods emerged as a potential alternative to the aforementioned traditional, mesh-based numerical methods. Nevertheless, meshless methods compared to FEM (which originated in the fifties) or FD (which date back even earlier) are still in their developement stages. In meshless methods no kind of a pre-defined nodal connectivity is necessary and, the nodes are uniformly or even non-uniformly distributed in the spatial domain and on the boundaries. As it is referred in [Belytschko, Krongauz, Organ, Fleming and Krysl (1996)], several meshfree methods have been proposed since the prototype of the meshfree methods, the Smoothed Particle Hydrodynamics (SPH), was born. Regarding the meshless methods, according to the formulation procedures they can be classified into two major categories, namely the collocation-based and the Galerkin-based methods, solving the strong- and weak-forms of the problems considered, respectively. Both formulations pose advantages and limitations [Liu and Gu (2005)].

Kansa [Kansa (1990)] introduced a numerical technique, in order to solve partial differential equations by collocation method using radial basis functions (RBFs). Since then, several radial basis functions introduced and Kansa's method has been further upgraded to symmetric collocation [Fasshauer (1997), Power and Barraco (2002)], to modified collocation [Chen (2002)], and to indirect collocation [Mai-

Duy and Tran-Cong (2003)]. We have to notice that the resulting collocation matrix obtained in Fasshauer's approach [Fasshauer (1997)] is symmetric and non-singular, while the matrix obtained in Kansa's approach is non-symmetric and in some cases non-singular. In spite of their accuracy, all of the above listed methods usually fail to perform on large problems, since they produce fully populated matrices, which are sensitive to the choice of the free parameters in RBFs. Furthermore, in all the cases mentioned above, a highly ill-conditioned dense matrix must be inverted due to the globally supported RBFs. Moreover, the computation complexity increases when these methods are applied at nonlinear or time dependent problems. Thus, these methods are impractical for real problems, where the nodes used and the resulting algebraic systems can be up to millions of unknowns.

On the other hand, sparse matrices can be generated by the introduction of the compactly supported RBFs. Thus, the concept of local collocation in the context of an RBF-based solution has been introduced by Wright and Fornberg [Wright and Fornberg (2006)]. As it is depicted, using the local RBFs some advantages are attained as, the only geometrical data needed for the construction of the matrices are for those nodes that fall into the support domain of each node, the properties of the constructed shape functions are the same with those for the global RBF, but the approximation method is stable and insensitive to the free parameter needed for the formulation and finally, the computational cost is decreasing since the matrix operations require the inversion of matrices of small size, equal to the number of nodes in the support domain [Wright and Fornberg (2006)].

For the construction of the meshless locally-supported shape functions, any Lagrangian or Hermitian RBF Hardy's interpolation can be used, which can reconstruct the field variable in each point into the support domain. Thus, several strategies have been proposed to possibly improve the imposing of the derivative boundary conditions in a strong-form approach. Some others efforts to bring localization in RBF-based methods have been independently made in [Lee, Liu and Fan (2003, Tolstykh and Shirobokov (2003), Šarler and Vertnik (2006), Vertnik and Šarler (2006)]. Particularly, numerical solutions for KdVB equation were obtained using sophisticated meshless numerical methods. In [Haq, Ul-Islam and Uddin (2009)] a simple classical radial basis functions (RBFs) collocation (Kansa) method was formulated for the numerical solution of the nonlinear dispersive and dissipative KdV–Burgers' (KdVB) equation.

In the present work the Inverse Multiquadrics (IMQ), Gaussian (GA) and Multiquadrics (MQ) Radial Basis Functions (RBF) interpolation are employed for the construction of the shape functions, not in the entire domain but in local subdomains, in conjunction with the general framework of the point collocation method in order to solve numerically the KdV-Burger equation and to depict the efficiency

and the accuracy of the proposed numerical scheme. Thus, first we solve the KdV-Burger equation by using the proposed numerical scheme, following we examine the numerical solution of the Burger's equation and, finally we turn to the well known KdV equation verifying the behavior of solitary waves. The rest of the paper is organized as follows. In Sections 2 and 3, we describe the interpolation method for the local sub-domains, which is used the main steps of the meshless point collocation numerical procedure. A stability analysis of the proposed numerical method is presented in Section 4, while numerical investigation for the KdV-Burger, Burger and KdV equations are presented in Section 5. Finally, our conclusions are given in Section 6.

2 Basic Concepts of Mesh Free Techniques

2.1 Defining the support domain

In the context of localized collocation meshless methods (LCMM), spatial discretization is performed over uniformly or non-uniformly distributed points, called nodes. Herein, the LCMM is handled with the local radial basis function formulation, where each node is connected to a set of neighboring points, defining a local topology of surrounding nodes, namely the support domain. The current local topology structure is fixed, that is, the number of nodes in the support domains remains constant. However, this structure can be altered based on the progress of the numerical solution, resulting in a local type refinement procedure.

2.2 Proposed numerical scheme

Consider a function $u(x)$ defined in the spatial domain Ω, represented by a set of nodes scattered in the problem domain and on the boundary $\partial\Omega$. The aforementioned function is then interpolated using the nodal values at the nodes of the support domain of a point of interest x_Q. Then, the approximation $u^h(x)$ of the function $u(x)$ at an arbitrary point x can be written, using the following finite series representation, as:

$$u^n(x_i) = \sum_{j=1}^{N} \lambda_j^n \varphi_i(r_{ij}), \tag{2}$$

where $x_i = i\delta x$, are collocation points in interval $[a,b]$, $i = 1,2,3,..,N$, δx is the space step, $r_{ij} = \left\|x_i - x_j\right\|$ is the distance between the collocation points x_i and x_j, and λ_j^n are unknown coefficients to be determined and $\phi(r_{ij})$ is a radial basis function, listed at Table 1. Following, we present the proposed collocation scheme to approximate the KdV-Burger's equation. We also present a θ-weighted time-

Table 1: Typical Conventional Form of Radial Basis Functions

Item	*Name*	*Expression*	**Shape Parameters**
1	Multiquadrics (MQ)	$R_i(x,y)=\left(r_i^2+C^2\right)^q=\left[(x-x_i)^2+(y-y_i)^2+C^2\right]^q$	C,q
2	Gaussian (GA)	$R_i(x,y)=e^{-cr_i^2}=e^{-c\left[(x-x_i)^2+(y-y_i)^2\right]}$	c
3	Thin plate splines (TPS)	$R_i(x,y)=r_i^\eta=\left[(x-x_i)^2+(y-y_i)^2\right]^\eta$	η
4	Logarithmic RBF	$R_i(r_i)=r_i^\eta \log r_i$	η
5	Inverse Multiquadrics (IQ)	$R_i(x,y)=\left(r_i^2+C^2\right)^{-q}=\left[(x-x_i)^2+(y-y_i)^2+C^2\right]^{-q}$	C,q

stepping scheme for temporal discretization. For that reason, we consider the KdV-Burger Eq. (1) subject to the Dirichlet boundary conditions,

$$u(a,t)=g_1(t), \quad u(b,t)=g_2(t), \quad t>0 \tag{3}$$

and initial condition,

$$u(x,0)=f(x), \quad x\in[a,b]\subset \mathbf{R}, \tag{4}$$

where g_1, g_2 are given functions of t and $f(x)$ is a bounded, localized disturbance inside the interval $[a,b]$. The discretization in time of Eq. (1) has been done using the Crank-Nicolson rule ($\theta=\frac{1}{2}$), while for the linearization of Eq. (1) the method of lagging the coefficients was applied. That is, for the linearization of the non-linear term $u\frac{\partial u}{\partial x}$, we assumed that the quantity u was locally constant, resulting in:

$$\frac{u^{n+1}-u^n}{\delta t}+\theta\left\{\varepsilon u^n u_x^{n+1}-\nu u_{xx}^{n+1}+\mu u_{xxx}^{n+1}\right\}+(1-\theta)\left\{\varepsilon u^n u_x^n-\nu u_{xx}^n+\mu u_{xxx}^n\right\}=0, \tag{5}$$

where $t^{n+1}=t^n+\delta t$, $u^{n+1}=u\left(x,t^{n+1}\right)$ and δt is the time step size.
Rearranging Eq. (5), we write the terms of the time step $(n+1)$ at the left hand side and the terms of the time step (n) at the right hand side, obtaining

$$u^{n+1}+\theta\delta t\left\{\varepsilon u^n u_x^{n+1}-\nu u_{xx}^{n+1}+\mu u_{xxx}^{n+1}\right\}=u^n-(1-\theta)\,\delta t\left\{\varepsilon u^n u_x^n-\nu u_{xx}^n+\mu u_{xxx}^n\right\}. \tag{6}$$

Following, we approximate the solution using RBF shape functions Eq. (2) and, substituting approximation Eq. (2) in Eq. (6) for all the interior points x_i, $i=$

$1,2,3,..,N-1$ we get the following discretized equation

$$\sum_{j=0}^{N}\lambda_j^{n+1}\varphi(r_{ij})+$$
$$\delta t\theta\left[\varepsilon\sum_{j=0}^{N}\lambda_j^{n}\varphi(r_{ij})\sum_{j=0}^{N}\lambda_j^{n+1}\varphi_x(r_{ij})-\nu\sum_{j=0}^{N}\lambda_j^{n+1}\varphi_{xx}(r_{ij})+\mu\sum_{j=0}^{N}\lambda_j^{n+1}\varphi_{xxx}(r_{ij})\right]=$$
$$\sum_{j=0}^{N}\lambda_j^{n}\varphi(r_{ij})-$$
$$\delta t(1-\theta)\left[\varepsilon\sum_{j=0}^{N}\lambda_j^{n}\varphi(r_{ij})\sum_{j=0}^{N}\lambda_j^{n}\varphi_x(r_{ij})-\nu\sum_{j=0}^{N}\lambda_j^{n}\varphi_{xx}(r_{ij})+\mu\sum_{j=0}^{N}\lambda_j^{n}\varphi_{xxx}(r_{ij})\right]. \tag{7}$$

Finally, the boundary conditions Eq. (3) become as

$$\sum_{j=0}^{N}\lambda_j^{n+1}\varphi(r_{0j})=g_1(t), \tag{8}$$

$$\sum_{j=0}^{N}\lambda_j^{n+1}\varphi(r_{Nj})=g_2(t). \tag{9}$$

Eq. (2) can be written in matrix notation

$$u^{(n)}(x_i)=\mathbf{A}\boldsymbol{\lambda}^{(n)}, \tag{10}$$

where $\mathbf{A}=[\varphi(r_{ij}):1\le i\le N,1\le j\le N]$ and $\boldsymbol{\lambda}^{(n)}=\left[\lambda_1^{(n)},\lambda_2^{(n)},...,\lambda_N^{(n)}\right]^T$. The matrix $\mathbf{A}$ can be split into two matrices $\mathbf{A}_d$ and $\mathbf{A}_b$ corresponding to $N-2$ interior points and two boundary points in the following form:

$$\mathbf{A}=\mathbf{A}_d+\mathbf{A}_b, \tag{11}$$

where $\mathbf{A}_d=[\varphi(r_{ij}):2\le i\le N-1,\ 1\le j\le N\ and\ 0\ elsewhere]$ and

$\mathbf{A}_b=[\varphi(r_{ij}):\ i=1,N,\ 1\le j\le N\ and\ 0\ elsewhere]$.

Finally, combining Eqs. (7)-(9) and (10) and writing in matrix notation we get

$$\begin{bmatrix}\mathbf{A}_d+\theta\delta t\left[\varepsilon\left(\mathbf{U}^{(n)}*\mathbf{B}_d\right)-\nu\mathbf{C}_d+\mu\mathbf{D}_d\right]\\ \mathbf{A}_b\end{bmatrix}\boldsymbol{\lambda}^{(n+1)}=$$
$$\begin{bmatrix}\mathbf{A}_d+\theta\delta t\left[\varepsilon\left(\mathbf{U}^{(n)}*\mathbf{B}_d\right)-\nu\mathbf{C}_d+\mu\mathbf{D}_d\right]\\ \mathbf{0}\end{bmatrix}\boldsymbol{\lambda}^{(n)}+\begin{bmatrix}0\\ \mathbf{g}^{(n+1)}\end{bmatrix}, \tag{12}$$

where $\mathbf{B}$, $\mathbf{C}$ and $\mathbf{D}$ are $(N-2)\times(N-2)$ matrices such that

$$\mathbf{B}=\left[\phi'(r_{ij}):2\le i\le N-1,\ \ 1\le j\le N \text{ and } 0 \text{ elsewhere}\right],$$

$$\mathbf{C}=\left[\phi''(r_{ij}):2\le i\le N-1,\ \ 1\le j\le N \text{ and } 0 \text{ elsewhere}\right],$$

$$\mathbf{D}=\left[\phi'''(r_{ij}):2\le i\le N-1,\ \ 1\le j\le N \text{ and } 0 \text{ elsewhere}\right].$$

The symbol $*$ means that the i^{th} component of the vector $\mathbf{U}^{(n)}$ is multiplied to every element of the i^{th} row of the matrix $\mathbf{B}$. Thus, Eq. (12) can be rewritten as

$$\boldsymbol{\lambda}^{(n+1)}=\mathbf{M}^{-1}\mathbf{N}\boldsymbol{\lambda}^{(n)}+\mathbf{M}^{-1}\mathbf{f}^{(n+1)}, \tag{13}$$

where

$$\mathbf{M}=\begin{bmatrix}\mathbf{A}_d+\theta\delta t\left[\varepsilon\left(\mathbf{U}^{(n)}*\mathbf{B}_d\right)-v\mathbf{C}_d+\mu\mathbf{D}_d\right]\\ \mathbf{A}_b\end{bmatrix},$$

$$\mathbf{N}=\begin{bmatrix}\mathbf{A}_d+\theta\delta t\left[\varepsilon\left(\mathbf{U}^{(n)}*\mathbf{B}_d\right)-v\mathbf{C}_d+\mu\mathbf{D}_d\right]\\ \mathbf{0}\end{bmatrix},$$

$$\mathbf{f}=\begin{bmatrix}0\\ \mathbf{g}^{(n+1)}\end{bmatrix},$$

From Eqs. (10) and (13), we can write

$$\mathbf{u}^{(n+1)}=\mathbf{A}\mathbf{M}^{-1}\mathbf{N}\mathbf{A}^{-1}\mathbf{u}^{(n)}+\mathbf{A}\mathbf{M}^{-1}\mathbf{f}^{(n+1)}. \tag{14}$$

Authors in [Hon and Schaback (2001)] have shown that the non-singularity of the matrix $\mathbf{M}$ can not be proved in general, therefore, it is not possible to show that the scheme is well-posed in all such cases. However, singularities in practical problems are rare. Eq. (14) represents a system of N linear algebraic equations in N unknown parameters u_j. A crucial point of the numerical method is the solution of the resulting algebraic problem. Since the positivity conditions [Jin, Li and Aluru (2004)] are fulfilled the resulting system can be solved by the Gaussian elimination method.

3 Stability Analysis

In this section, we present the stability of the Eq. (14) considering the local meshless approximation using the matrix method. As we already mentioned, Eq. (1) can

be linearized by assuming the quantity u in the nonlinear term $u\frac{\partial u}{\partial x}$ in Eq. (6) as locally constant. The error $e^{(n)}$ at the n^{th} time level is given by

$$e^{(n)} = u_{exact}^{(n)} - u_{app}^{(n)}, \tag{15}$$

where $u_{exact}^{(n)}$ and $u_{app}^{(n)}$ are the exact and the numerical solutions at the nth time level. The error equation for the linearized KdVB equation, in matrix form, can be written as;

$$\mathbf{e}^{n+1} = \mathbf{K}\mathbf{e}^{n}, \tag{16}$$

where the amplification matrix $\boldsymbol{K}$ is

$$\mathbf{K} = \left[\mathbf{A}_d + \theta\delta t\left[\varepsilon\left(\mathbf{U}^{(n)} * \mathbf{B}_d\right) - \nu\mathbf{C}_d + \mu\mathbf{D}_d\right]\right]^{-1}\left[\mathbf{A}_d + \frac{\delta t}{2}\left[-\mu\mathbf{D}_d + \nu\mathbf{C}_d\right]\right]. \tag{17}$$

The numerical scheme will be stable as $n \to \infty$ if the error $e^n \to 0$. This can be guaranteed provided that $\|\mathbf{K}\|_2 \leq 1$, which is equivalent to $\rho(\mathbf{K}) < 1$, where $\rho(\mathbf{K})$ denotes the spectral radius of the amplification matrix $\mathbf{K}$. From Eq. (17), it can be seen that the stability is assured if all the eigenvalues of the matrix

$$K = \left[\mathbf{H} + \theta\delta t\mathbf{J}\right]^{-1}\left[\mathbf{H} - (1-\theta)\delta t\mathbf{J}\right] \tag{18}$$

satisfy the following condition

$$\left|\frac{\lambda_H - \delta t(1-\theta)\lambda_J}{\lambda_H + \delta t\theta\lambda_J}\right| \leq 1, \tag{19}$$

where $\mathbf{H} = \mathbf{A}_d$, $\mathbf{J} = -\nu\mathbf{C}_d + \mu\mathbf{D}_d$ and λ_H, λ_J are the eigenvalues of the matrix $\mathbf{H}$ and $\mathbf{J}$, respectively. When $\theta = 0.5$, the above inequality becomes

$$\left|\frac{\lambda_H - 0.5\delta t\lambda_J}{\lambda_H + 0.5\delta t\lambda_J}\right| \leq 1. \tag{20}$$

In case of complex eigenvalues $\lambda_H = a_h + ib_h$, $\lambda_J = a_j + ib_j$, where a_h, a_j, b_h and b_j are any real numbers, the inequality Eq. (20) takes the following form,

$$\left|\frac{(a_h - 0.5\delta ta_J) + i(b_h - 0.5\delta tb_J)}{(a_h + 0.5\delta ta_J) + i(b_h + 0.5\delta tb_J)}\right| \leq 1. \tag{21}$$

The inequality Eq. (21) is satisfied if $a_h a_j + b_h b_j \geq 0$. For real eigenvalues, the inequality Eq. (21) holds true if either ($\lambda_H \geq 0$ and $\lambda_J \geq 0$) or ($\lambda_H \leq 0$ and $\lambda_J \leq 0$).

This shows that the scheme Eq. (21) is unconditionally stable if $a_h a_j + b_h b_j \geq 0$, for complex eigenvalues and if either ($\lambda_H \geq 0$ and $\lambda_J \geq 0$) or ($\lambda_H \leq 0$ and $\lambda_J \leq 0$), for real eigenvalues. When $\theta = 0$, the inequality Eq. (19) becomes

$$\left|1 - \frac{\delta t \lambda_J}{\lambda_H}\right| \leq 1. \tag{22}$$

Thus for $\theta = 0$, the scheme is conditionally stable. The stability of the scheme and conditioning of the component matrices **H**, **J** depend on the weight parameter θ, the minimum distance between any two collocation points h in the domain set $[a,b]$ and the shape parameter c. Authors in [Cheng, Golberg, Kansa and Zammito (2003)] showed that when c is very large then the RBFs system error is of exponential order. But there is a certain limit for the value c after which the solution breaks down. For the limiting value of c the condition number of the RBFs system becomes so large that the system leads to ill-conditioning. In the case of an ill-conditioned system, the numerical solution thus produced is not stable.

4 Numerical results

In this section we investigate numerically the behavior of the KdV-Burger's equation and for that reason we solve three representative examples in order to check the efficiency and the validity of the proposed scheme. Thus, accuracy of the results is computed using the L_2 and the L_∞ error norms given by

$$L_2 = \|u_{exact} - u_{app}\|_2 = \sqrt{h \sum_{j=0}^{N} \left|(u_{exact})_j - (u_{app})_j\right|^2}, \tag{23}$$

and

$$L_\infty = \|u_{exact} - u_{app}\|_\infty = \max_j \left|(u_{exact})_j - (u_{app})_j\right|, \tag{24}$$

where u_{exact} and u_{app} represent the exact and approximate solutions respectively and h the minimum grid spacing. Concerning the conservation properties, the KdV-Burger's equation possesses three conservative properties related to mass, momentum and energy given by [Miura, Gardner and Kruskal (1968)]

$$C_1 = \int_a^b u dx, \tag{25}$$

$$C_2 = \int_a^b u^2 dx, \tag{26}$$

$$C_3 = \int_a^b \left(u^3 - \frac{3\mu}{\varepsilon} (u_x)^2 \right) dx. \tag{27}$$

In order to achieve accurate results a comprehensive study took place, regarding the total number of the nodes used, the number of nodes in the support domain of each center node, the shape parameter used and, finally the condition number of the moment matrix. A compromise between the condition number and the shape parameter was chosen in order to fulfill the requirements of the so-called 'Schaback uncertainty condition' [Hon and Schaback (2001)]. We can observe that the local RBF methods can give accurate numerical result, but they are very sensitive to the choice of the shape parameter used at the shape functions. More precisely we define the condition number of the moment matrix as a criterion, combining all the above parameters that produces accurate, efficient and stable numerical results. Thus, we examine the efficiency and the accuracy of the proposed scheme using three representative numerical examples.

4.1 Example 1: KdV-Burger's

Consider KdV-Burger's equation and the initial condition

$$u(x,0) = -\frac{6\nu^2}{25\mu} \left[1 + \tanh\left(\frac{\nu x}{10\mu} \right) + \frac{1}{2} \sec h^2 \left(\frac{\nu x}{10\mu} \right) \right]. \tag{28}$$

The exact solution, having initial condition (Eq. (28)) is given by [Kaya (2004)]

$$u(x,t) = -\frac{6\nu^2}{25\mu} \left[1 + \tanh(\xi) + \frac{1}{2} \sec h^2(\xi) \right], \tag{29}$$

where $\xi = \frac{\nu}{10\mu} \left(x + \frac{6\nu^2}{25\mu} t \right)$. Additionally, we consider the following boundary conditions

$$u(\alpha,t) = -\frac{6\nu^2}{25\mu} \left[1 + \tanh\left(\frac{\nu}{10\mu} \left(\alpha + \frac{6\nu^2}{25\mu} t \right) \right) + \frac{1}{2} \sec h^2 \left(\frac{\nu}{10\mu} \left(\alpha + \frac{6\nu^2}{25\mu} t \right) \right) \right], \tag{30}$$

$$u(b,t) = -\frac{6\nu^2}{25\mu} \left[1 + \tanh\left(\frac{\nu}{10\mu} \left(b + \frac{6\nu^2}{25\mu} t \right) \right) + \frac{1}{2} \sec h^2 \left(\frac{\nu}{10\mu} \left(b + \frac{6\nu^2}{25\mu} t \right) \right) \right]. \tag{31}$$

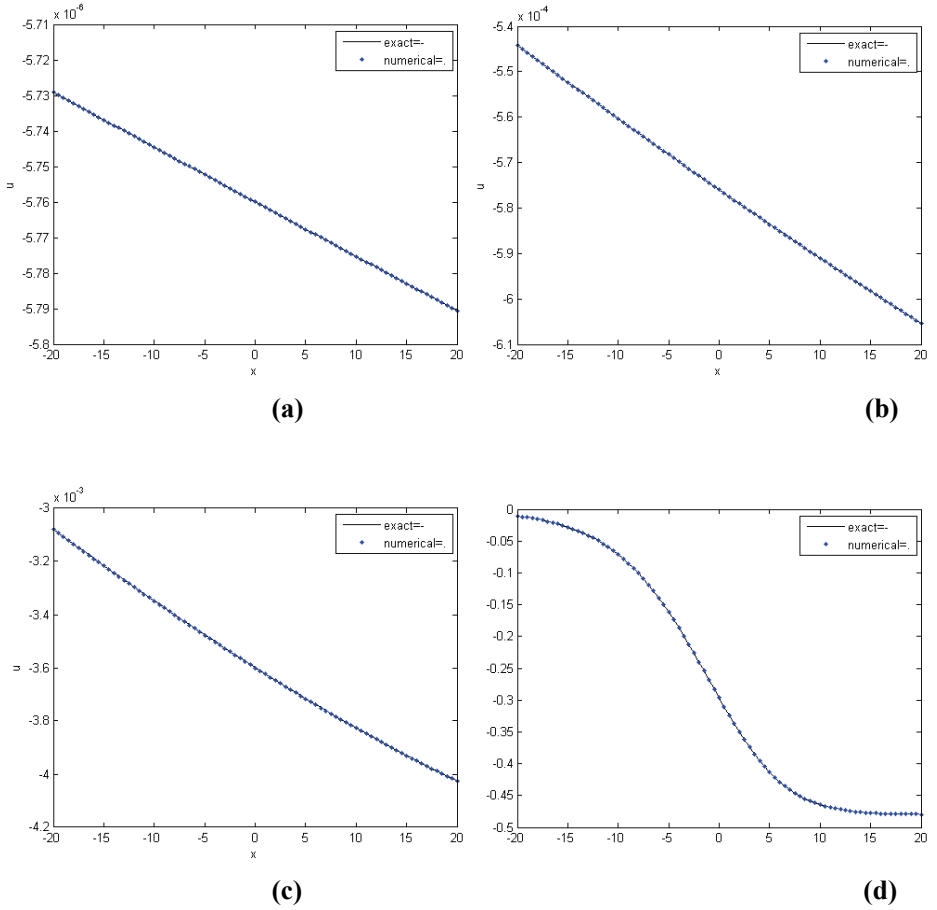

Figure 1: KdVB type solutions for different values of the viscosity (a) ν =0.004 - (b) ν =0.04 - (c) ν =0.1 and (d) ν =1 , showing that solution vector for KdVB equation tends to behave like a solution of Burger equation, when local type MQ shape function is used.

Furthermore, for our computations we consider $\varepsilon = 1$, $\mu = 0.1$, $\delta x = 0.5$, $\delta t = 0.01$ and $\nu = 0.004, 0.04, 0.1$ respectively, in order to study the effects of viscosity in Eq. (1). The spatial domain is defined as $-20 \leq x \leq 20$. In Fig. 1, the solution profiles for different values of ν are presented and, the numerical results are plotted using the local type MQ shape function, and are compared with the analytical solution. From the figures presented we can observe that, as viscosity ν increases the solution of KdVB equation tends to behave like the solution of Burgers' equation (Example

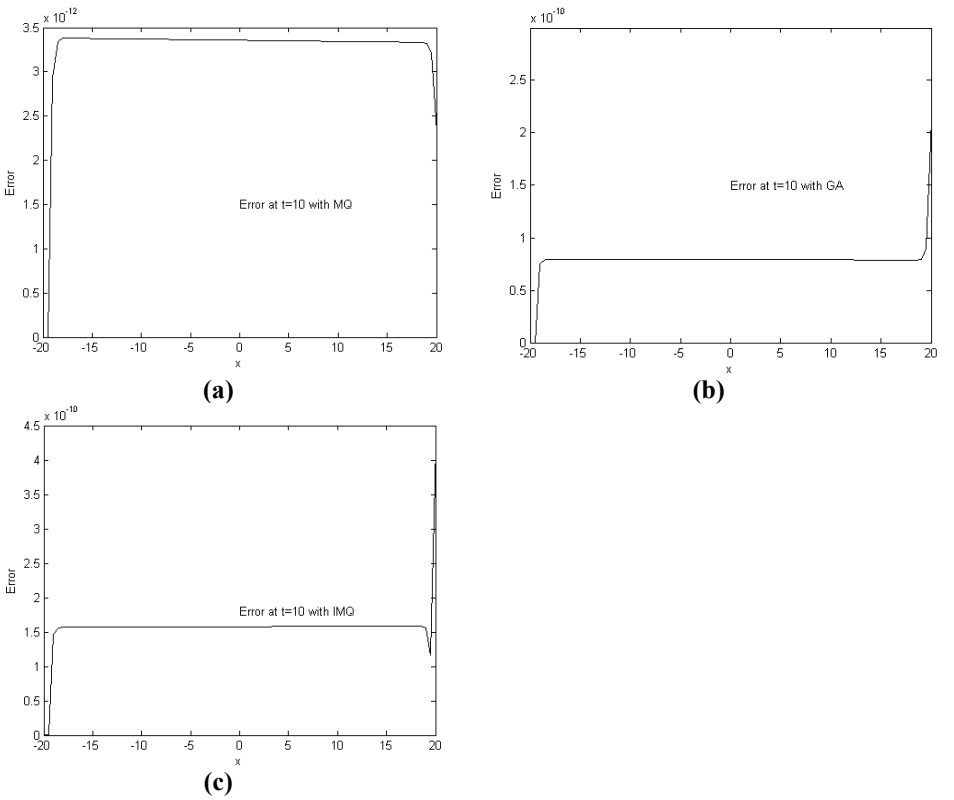

Figure 2: Errors (exact solution-numerical solution) at t = 10 for v =0.004.

2), since the solution describes a formatting steep layer. Furthermore, Fig. 2 represents the error graphs of the solutions at time $t = 10s$ using local IMQ, MQ, and GA, respectively.

The L_2 and L_∞ error norms, and the conservative laws are shown in Tables 2–4. The numerical results obtained using the global RBF functions are listed in Tables 2a-3a-4a, while the results from local RBF in Tables 2b-3b-4b. The numerical results listed there show that all the three invariants are preserved very accurately by the local meshfree method. Numerical results obtained using three types of radial basis functions, i.e., global multiquadric (MQ), Gaussian (GA) and Inverse quadric (IMQ) are compared with the results provided herein using the local type RBF functions. Concerning the local RBF functions, the tabulated results obtained corresponding to the values of shape parameter $c = 0.005$, $c = 0.025$ and $c = 0.01$ for LMQ, LGA and LIQ, respectively. The support domain was defined to be the

Table 2a: Invariants and error norms for single soliton v = 0.004 and δt = 0.001 , using global RBF.

Time	1s	2s	3s	10s
MQ				
C_1	-2.331E-003	-2.331E-003	-2.331E-003	-2.331E-003
C_2	1.343E-007	1.343E-007	1.343E-007	1.343E-007
C_3	-8.619E-012	-8.622E-012	-8.624E-012	-8.630E-012
L_∞	6.822E-009	1.150E-008	1.485E-008	2.479E-008
L_2	8.845E-009	1.652E-008	2.338E-008	6.046E-008
GA				
C_1	-2.360E-003	-2.360E-003	-2.360E-003	-2.364E-003
C_2	1.360E-007	1.360E-007	1.360E-007	1.364E-007
C_3	-8.137E-012	-8.195E-012	-8.451E-012	-2.161E-011
L_∞	7.913E-009	5. 128E-008	1.677E-007	3.294E-006
L_2	5.378E-009	3.488E-008	1.199E-007	3.706E-006
IQ				
C_1	-2.331E-003	-2.331E-003	-2.332E-003	-2.332E-003
C_2	1.343E-007	1.343E-007	1.344E-007	1.344E-007
C_3	-9.202E-012	-1.148E-011	-1.368E-011	-2.161E-011
L_∞	4.077E-007	7.475E-007	9.830E-007	1.270E-006
L_2	2.574E-007	4.982E-007	6.709E-007	8.858E-007

Table 2b: Invariants and error norms for single soliton v =0.004 and δt =0.01 , using local RBF.

Time	1s	2s	3s	10s
LMQ				
C_1	-2,103E-004	-2.304E-004	-2.304E-004	-2.304E-004
C_2	1.327E-009	1.327E-009	1.327E-009	1.327E-009
C_3	-7.644E-015	-7.644E-015	-7.644E-015	-7.644E-015
L_∞	3.293E-013	6.585E-013	9.877E-013	3.292E-012
L_2	2.048E-012	4.094E-012	6.140 E-012	2.043E-011
LGA				
C_1	-2.303E-004	-2.303E-004	-2.303E-004	-2.303E-004
C_2	1.327E-009	1.327E-009	1.327E-009	1.327E-009
C_3	-7.644E-015	-7.644E-015	-7.644E-015	-7.644E-015
L_∞	7.953E-012	1.590E-011	2.386E-011	7.952E-011
L_2	4.977E-011	9.952E-011	1.492E-010	4.969E-010
LIMQ				
C_1	-2.303E-004	-2.303E-004	-2.303E-004	-2.303E-004
C_2	1.327E-009	1.327E-009	1.327E-009	1.327E-009
C_3	-7.644E-015	-7.644E-015	-7.644E-015	-7.644E-015
L_∞	1.586E-011	3.172E-011	4.759E-011	1.586E-010
L_2	9.908E-011	1.981E-010	2.971E-010	9.892E-010

Table 3a: Invariants and error norms for single soliton v =0.04 and δt =0.001

Time	1s	2s	3s	10s
MQ				
C_1	-2.198E-001	-2.198E-001	-2.199E-001	-2.200E-001
C_2	1.300E-003	1.300E-003	1.300E-003	1.301E-003
C_3	-8.368E-006	-8.369E-006	-8.371E-006	-8.381E-006
L_∞	2.936E-006	4.204E-006	4.126E-006	5.800E-006
L_2	3.727E-007	2.207E-008	1.928E-006	1. 297E-005
GA				
C_1	-2.223E-001	-2.223E-001	-2.223E-001	-2.229E-001
C_2	-1.315E-003	-1.315E-003	-1.316E-003	-1.323E-003
C_3	-8.477E-006	-8.481E-006	-8.491E-006	-8.654E-006
L_∞	-1.482E-006	-8.668E-006	2.665E-005	2.987E-004
L_2	2.865E-006	9.908E-006	2.575E-005	4.084E-004
IQ				
C_1	-2.198E-001	-2.200E-001	-2.202E-001	-2.186E-001
C_2	1.300E-003	1.302E-003	1.304E-003	1.284E-003
C_3	-8.381E-006	-8.592E-006	-8.545E-006	-1.349E-005
L_∞	3.925E-005	2.465E-004	3.567E-004	1.669E-003
L_2	2.842E-005	2.251E-004	4.205E-004	1.878E-003

Table 3b: Invariants and error norms for single soliton v =0.04 and δt =0.01

Time	1s	2s	3s	10s
LMQ				
C_1	-0.230E-002	-0.230E-002	-0.230E-002	-0.230E-002
C_2	1.326E-005	1.326E-005	1.326E-005	1.326E-005
C_3	-7.649E-009	-7.649E-009	-7.649E-009	-7.649E-009
L_∞	1.645E-009	3.284E-009	4.919E-009	1.638E-008
L_2	9.529E-009	1.900E-008	2.844E-008	9.375E-008
LGA				
C_1	-0.230E-002	0.230E-002	0.230E-002	0.230E-002
C_2	1.326E-005	1.326E-005	1.326E-005	1.326E-005
C_3	-7.649E-009	-7.649E-009	-7.649E-009	-7.649E-009
L_∞	7.679E-009	1.535E-008	2.300E-008	7.643E-008
L_2	4.515E-008	9.016E-008	1.350E-007	4.469E-007
LIQ				
C_1	-0.230E-002	-0.230E-002	-0.230E-002	-0.230E-002
C_2	1.326E-005	1.326E-005	1.326E-005	1.326E-005
C_3	-7.649E-009	-7.649E-009	-7.649E-009	-7.649E-009
L_∞	1.175E-009	2.342E-009	3.507E-009	1.156E-008
L_2	5.707E-009	1.139E-008	1.706E-008	5.645E-008

Table 4a: Invariants and error norms for single soliton v =0.1 and δt =0.001

Time	1s	2s	3s	10s
MQ				
C_1	-1.205E-000	-1.206E-000	-1.207E-000	-1.215E-000
C_2	4.863E-002	4.868E-002	4.874E-002	4.912E-002
C_3	-2.150E-003	-2.152E-003	-2.155E-003	-2.172E-003
L_∞	1.540E-005	3. 760E-005	4.604E-005	1.498E-004
L_2	1.004E-005	1.732E-005	2.874E-005	1.342E-004
GA				
C_1	-1.217E-000	-1.218E-000	-1.220E-000	-1.228E-000
C_2	4.921E-002	4.926E-002	4.933E-002	4.979E-002
C_3	-2.178E-003	-2.181E-003	-2.184E-003	-2.207E-003
L_∞	1.540E-005	6.794E-005	1.622E-004	4.886E-004
L_2	2.564E-005	8.394E-005	1.864E-004	1.058E-003
IQ				
C_1	-1.205E-000	-1.206E-000	-1.207E-000	-1.216E-000
C_2	4.863E-002	4.870E-002	4.876E-002	4.919E-002
C_3	-2.151E-003	-2.154E-003	-2.156E-003	-2.178E-003
L_∞	1.314E-004	2.330E-004	1.741E-004	4.436E-004
L_2	1.169E-004	3.476E-004	3.315E-004	1.218E-003

Table 4b: Invariants and error norms for single soliton v =0.1 and δt =0.01

Time	1s	2s	3s	10s
LMQ				
C_1	-1.434E-001	-1.434E-001	-1.434E-001	-1.434E-001
C_2	5,169E-004	5,169E-004	5,169E-004	5,169E-004
C_3	-1,874E-006	-1,874E-006	-1,874E-006	-1,874E-006
L_∞	2.054E-007	4.094E-007	6.126E-007	2.016E-006
L_2	1.097E-006	2.184E-006	3.265E-006	1.068E-005
LGA				
C_1	-1.434E-001	-1.434E-001	-1.434E-001	-1.434E-001
C_2	5,169E-004	5,169E-004	5,169E-004	5,169E-004
C_3	-1,874E-006	-1,874E-006	-1,874E-006	-1,874E-006
L_∞	2.428E-007	4.847E-007	7.256E-007	2.400E-006
L_2	1.314E-006	2.620E-006	3.921E-006	1.291E-005
LIMQ				
C_1	-1.434E-001	-1.434E-001	-1.434E-001	-1.434E-001
C_2	5,169E-004	5,169E-004	5,169E-004	5,169E-004
C_3	-1,874E-006	-1,874E-006	-1,874E-006	-1,874E-006
L_∞	1.543E-007	3.078E-007	4.606E-007	1.522E-006
L_2	8.151E-007	1.625E-006	2.431E-006	8.006E-006

two nearest nodes, defining a stencil of three nodes, the central and the two neighbors. The condition number was 1.5360×10^{11}, 1.2288×10^{8} and 4.8004×10^{9} respectively.

We can observe that the local type of interpolations scheme posses better accuracy than the global one. More precisely, among the interpolation methods used, local MQ is the most accurate. We have to notice that the time step used is one order less than that used in [Haq, Ul-Islam and Uddin (2009)], obtaining a more efficient numerical scheme, since the time steps used is less, one order lower.

4.2 Example 2: Burger equation

By taking $\mu = 0$, $v = 1$ and $\varepsilon = 1$ the KdVB equation reduces to Burger equation defined as

$$\frac{\partial u}{\partial t} + u\frac{\partial u}{\partial x} - v\frac{\partial^2 u}{\partial x^2} = 0 \tag{32}$$

and subject to the initial condition

$$u(x,0) = \frac{\alpha + \beta + (\beta - \alpha)\, e^{\gamma}}{1 + e^{\gamma}}, \tag{33}$$

where $\gamma = \left(\frac{\alpha}{v}\right)(x - \eta)$ and α, β, η, v are the parameters. The exact solution [Kaya (2004)] of the above problem is given by

$$u(x,t) = \frac{\alpha + \beta + (\beta - \alpha)\, e^{\zeta}}{1 + e^{\zeta}}, \tag{34}$$

where $\zeta = \left(\frac{\alpha}{v}\right)(x - \beta t - \eta)$.

For the numerical computations we choose $\alpha = 0.4$, $\beta = 0.6$, $\eta = 0.125$, $\delta x = 0.2$ and $\delta t = 0.01$ in order to compare our results with those given in [Zaki (2000)] and [Haq, Ul-Islam and Uddin (2009)]. We solve the Burger equation (Eq. (32)) with initial condition (Eq. (33)) using the localized form of the radial basis functions (MQ, GA, IQ) and compare the numerical results with those obtained using the global form of the aforementioned radial basis functions. The L_∞ and L_2 error norms are computed and are given in Table 5a for global RBF and in Table 5b for local RBF. It can be seen that the local RBF are also accurate as the global ones, even though we use a time step $\delta t = 0.01$, while in [Zaki (2000)] and [Haq, Ul-Islam and Uddin (2009)] a time step $\delta t = 0.001$ has been used. In Fig. 3, we display the exact and numerical solution using the local IQ shape functions, whereas Fig. 4 represents the error graphs of the solutions with local MQ, GA and IQ, respectively, at time $t = 1$. The tabulated results obtained corresponding to the

Table 5a: Error norms for single soliton using global RBFs.

Time	0.1	0.3	0.5	0.8	1.0
MQ					
L_∞	1.064E-005	1.292E-005	1.449E-005	2.082E-004	2.497E-005
L_2	1.926E-005	3.979E-005	5.523E-005	7.480E-005	8.654E-005
GA					
L_∞	1.220E-003	3.686E-003	6.166E-003	9.956E-003	1.251E-002
L_2	1.338E-005	7.503E-005	2.028E-004	5.464E-004	8.601E-004
IQ					
L_∞	1.22E-003	3.686E-003	6.166E-003	9.956E-003	1.251E-002
L_2	2.597E-006	1.254E-005	2.865E-005	6.361E-005	9.321E-005

Table 5b: Error norms for single soliton using local RBFs.

Time	0.1	0.3	0.5	0.8	1.0
LMQ					
L_∞	4.753E-003	1.428E-002	2.381E-002	3.806E-002	4.762E-002
L_2	1.234E-002	3.703E-002	6.173E-002	9.876E-002	1.234E-001
LGA					
L_∞	1.727E-005	5.043E-005	8.266E-005	1.288E-004	1.574E-004
L_2	3.504E-005	1.033E-004	1.694E-004	2.648E-004	3.259E-004
LIQ					
L_∞	1.804E-005	5.278E-005	8.646E-005	1.350E-004	1.652E-004
L_2	3.577E-005	1.055E-004	1.732E-005	2.708E-004	3.335E-004

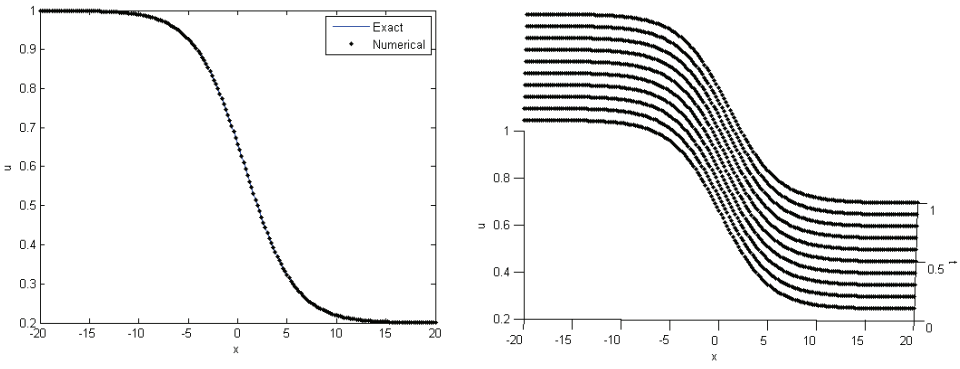

Figure 3: Solution graph of Burgers' equation, when local type IQ shape function is used.

values of shape parameter $c = 0.005$, $c = 0.025$ and $c = 0.01$ for LMQ, LGA and LIQ, respectively. The support domain was defined to be the two nearest nodes, defining a stencil of three nodes, the central and the two neighbors. The condition number was 1.5360×10^{11}, 1.2288×10^{8} and 4.8004×10^{9} respectively.

We can observe that for global RBFs, MQ approximation obtains better accuracy than that of GA and IQ, while for local type RBfs GA posses better accuracy compared to MQ and IQ, and the L_∞ error norm is bigger compared of that of global MQ.

4.3 Example 3: KdV equation

By taking $\mu = 1$, $\nu = 0$ and $\varepsilon = -6$ the KdVB equation reduces to KdV equation, defined as

$$\frac{\partial u}{\partial t} - 6u\frac{\partial u}{\partial x} + \frac{\partial^3 u}{\partial x^3} = 0 \tag{35}$$

and subject to the initial condition

$$u(x,0) = -2\sec h^2(x). \tag{36}$$

The exact solution [Kaya (2004)] of the above problem is given by

$$u(x,t) = -2\sec h^2(x-4t). \tag{37}$$

The KdV equation represents an approximation in the study of long wavelength, small amplitude inviscid and incompressible fluids. Since the formulation of the

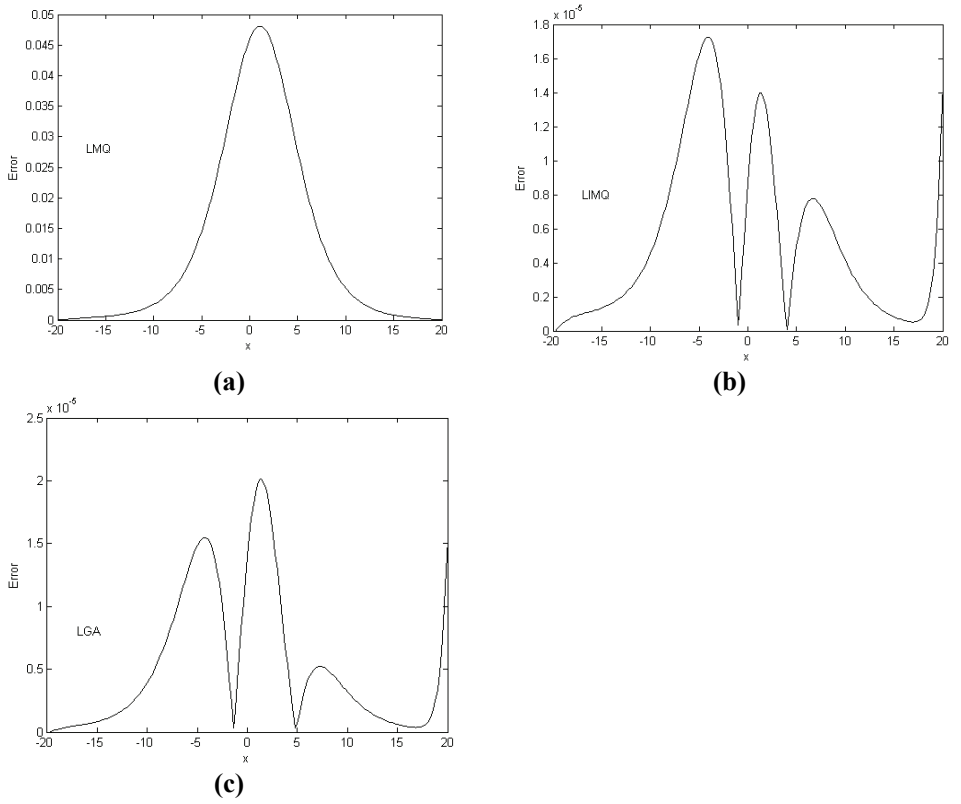

Figure 4: Error (exact-numerical) at t = 1 of Burgers' equation.

KdV equation, numerous researches have been worked over its analytical solution. However, a wide class of solutions of this equation was difficult to obtain due to its non-linearity. Due to its inherent difficulty, numerical solutions are used. We combine meshless point collocation in space and a finite difference scheme in time to investigate numerically interactions of solitary wave solutions of the KdV equation.

Herein, for the numerical computations we choose $\delta x = 0.2$ and $\delta t = 0.01$ in order to compare our results with those given in [Zaki (2000)] and [Haq, Ul-Islam and Uddin (2009)]. We solve the KdV equation (35) with initial condition (36) using the localized form of the radial basis functions MQ, GA and IQ and compare the numerical results with those obtained using the global form of the aforementioned radial basis functions. The L_∞ and L_2 error norms are computed and are given in Table 6a for global RBF and in Table 6b for local RBF. It can be seen that the local RBF are more accurate than the global ones, in some cases one or even two orders

Table 6a: Invariants and error norms for single soliton.

Time	C_1	C_2	C_3	L_∞	L_2
MQ					
0.1	-4.000	5.333	-6.400	2.024E-003	9.966E-007
1	-4.000	5.333	-6.400	9.855E-004	1.088E-004
2	-4.000	5.333	-6.400	1.096E-003	3.405E-004
3	-4.000	5.333	-6.400	9.016E-004	3.445E-005
GA					
0.1	-4.000	5.333	-6.400	2.023E-003	1.152E-005
1	-4.000	5.333	-6.400	9.512E-004	1.688E-004
2	-4.000	5.333	-6.400	1.194E-003	2.842E-004
3	-4.000	5.333	-6.400	8.000E-004	4.844E-004
IQ					
0.1	-4.000	5.333	-6.400	2.024E-003	6.275E-005
1	-4.000	5.333	-6.400	9.730E-004	1.077E-003
2	-4.000	5.333	-6.400	1.270E-003	3.607E-003
3	-4.000	5.333	-6.400	2.688E-003	1.026E-002

Table 6b: Invariants and error norms for single soliton.

Time	C_1	C_2	C_3	L_∞	L_2
LMQ					
0.1	-4.000	5.333	-6.400	3.142E-004	7.866E-007
1	-4.000	5.333	-6.400	9.365E-005	1.188E-005
2	-4.000	5.333	-6.400	1.054E-004	4.455E-005
3	-4.000	5.333	-6.400	9.316E-005	2.127E-006
LGA					
0.1	-4.000	5.333	-6.400	3.443E-004	1.004E-005
1	-4.000	5.333	-6.400	8.462E-005	1.188E-004
2	-4.000	5.333	-6.400	2.194E-004	2.142E-004
3	-4.000	5.333	-6.400	7.125E-005	3.844E-004
LIQ					
0.1	-4.000	5.333	-6.400	1.324E-004	2.455E-005
1	-4.000	5.333	-6.400	7.730E-005	1.277E-004
2	-4.000	5.333	-6.400	4.270E-004	2.637E-004
3	-4.000	5.333	-6.400	2398E-004	1.426E-004

of magnitude accurate using a time step $\delta t = 0.01$ while in [Zaki (2000)] and [Haq, Ul-Islam and Uddin (2009)] a time step $\delta t = 0.001$ was used.

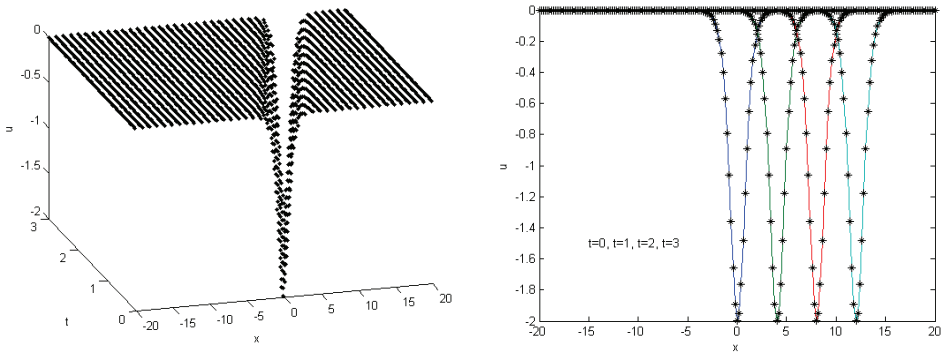

(a) **(b)**

Figure 5: Motion of solitary wave at t =0–3 .

In Fig. 5, numerical and exact solutions are plotted on the same diagram which shows an excellent agreement. It is clear from the figure that as the time increases the solution moves towards the right with a constant speed. The difference between the exact and numerical solutions (error) are plotted in Fig. 6 for the three methods when $t = 0$ up to $t = 3$.

5 Conclusions

We have applied the localized meshless collocation method using three standard RBFs, that is, MQ, GA and IQ for the numerical solution of nonlinear KdV–Burgers' equation and, we compared the numerical results with those obtained using the global RBFs. The KdV–Burgers' equation models physical problems such as irrotational incompressible flow, considering a shallow layer of an inviscid fluid moving under the influence of gravity and the motion of solitary waves. The results show that this scheme is an efficient approach for the solution of such type of nonlinear equations and, more precisely, the local type gives more accurate results from the global one, even with larger time step ($\delta t = 0.001$ and $\delta t = 0.01$ for global and local type respectively). It is noted that time marching process reduces the solution accuracy due to the time truncation errors. As far as its application is concerned we have found that RBFs method is very much simple and straightforward, irrespective of the dimension and geometry of the problem. Thus, we have avoided the use of fully populated matrices that are created in case of global RBFs.

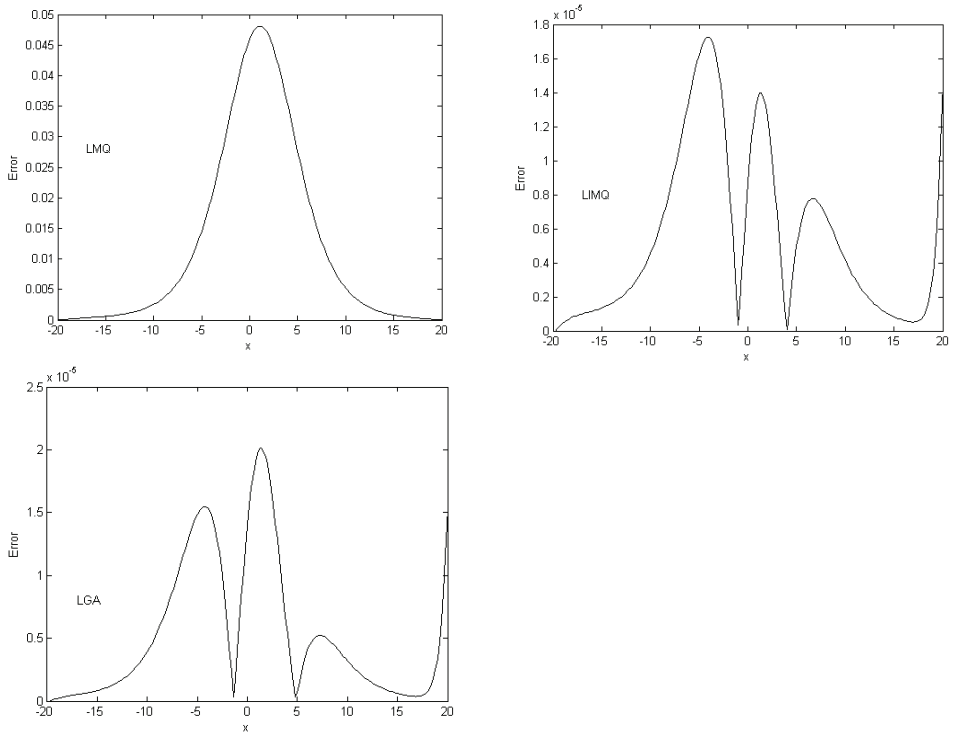

Figure 6: Error (exact-numerical) at t =3 of KdV equation.

The stability analysis presented shows that the proposed numerical scheme is stable. Furthermore, the accuracy of the method was assessed in terms of the L_2 and L_∞ error norms and three conservative properties related to mass, momentum and energy.

References

Antar, N., Demiray, H. (1997): Nonlinear waves in an inviscid fluid contained in an pre-stressed thin viscoelastic tube. *ZAMP*, vol. 48, pp. 325-340.

Atluri, S. N, Shen, S. P. (2002): The Meshless Local Petrov–Galerkin (MLPG) Method. Tech Science Press, Encino USA.

Belytschko, T., Krongauz, Y., Organ, D., Fleming, M., Krysl, P. (1996): Meshless methods: an overview and recent developments, *Computer Methods in Applied Mechanics and Engineering*, vol. 139, pp. 3-47.

Burger, J. M. (1939): Mathematical examples illustrating relations occurring in the

theory of turbulent fluid motion. *Transactions of the Royal Netherlands Academy Science, Amsterdam*, vol. 17, pp. 1-53.

Chen, W. (2002): New RBF collocation schemes and kernel RBFs with applications. *Lecture Notes in Computational Science and Engineering*, vol. 26, pp. 75-86.

Cheng, A. H. D., Golberg, M. A., Kansa, E. J., Zammito, G. (2003): Exponential convergence and H-c multiquadric collocation method for partial differential equations. *Numerical Methods for Partial Differential Equations*, vol. 19, pp. 571-594.

Demeiray, H. (1998): Nonlinear waves in a thick walled viscoelastic tube filled with an inviscid fluid. *International Journal of Engineering Science*, vol. 36, pp. 359-362.

Fasshauer, G. (1997): Solving partial differential equations by collocation with radial basis functions. *In Surface Fitting and Multiresolution Methods*. (Edited by A.L. Mehaute, C. Rabut and L.L. Schumaker).

Grad, H., Hu, P. N. (1967): Unified shock profile in a plasma. *Physics of Fluids*, vol. 10, pp. 2596-2601.

Haq, S., Ul-Islam, S., Uddin, M. (2009): A mesh-free method for the numerical solution of the KdV–Burgers equation. *Applied Mathematical Modelling*, vol. 33, pp. 3442-3449.

Hon, Y. C., Schaback, R. (2001): On unsymmetric collocation by radial basis functions. *Applied Mathematics and Computation*, vol. 119, pp. 177-186.

Jin, X., Li, G., Aluru, N. R. (2004): Positivity conditions in meshless collocation methods. *Computer Methods in Applied Mechanics and Engineering*, vol. 193, pp. 1171-1202.

Jonson, R. S. (1970): A non-linear equation incorporating damping and dispersion. *Journal of Fluid Mechanics*, vol. 42, pp. 49-60.

Kansa, E. J. (1990): Multiquadrics scattered data approximation scheme with applications to computational fluid-dynamics. I. Surface approximations and partial derivative estimates. *Applied Mathematics and Computation*, vol. 19, pp. 127-145.

Kaya, D. (2004): An application of the decomposition method for the KdVB equation. *Applied Mathematics and Computation*, vol. 152, pp. 279-288.

Kaya, D., Aassila, M. (2006): Decomposition method for the solution of the nonlinear Kortewege-de Vries equation., *Physics Letters A*, vol. 299, pp. 201-206.

Kortewege, D. J., de Vries, G. (1895): On the change of form of long waves advancing in a rectangular channel and on a new type of long stationary waves. *Philosophical Magazine*, vol. 39, pp. 422-443.

Lee, C. K., Liu, X., Fan, S. C. (2003): Local multiquadric approximation for solving boundary value problems. *Computational Mechanics*, vol. 30, pp. 396-409.

Liu, G. R. (2002): Mesh Free Methods, Moving beyond the Finite Element Method. CRC Press.

Liu, G. R., Gu, Y. T. (2005): An introduction to meshfree methods and their programming. Springer. The Netherlands.

Mai-Duy, N., Tran-Cong, T. (2003): Indirect RBPN method with thin plate splines for numerical solution of differential equations. *CMES: Computer Modeling in Engineering & Sciences*, vol. 4, pp. 85-102.

Miura, R. M., Gardner, G. S., Kruskal, M. D. (1968): Kortewege-de Vries equation and generalization. II. Existence of conservation laws and constants of motion. *Journal of Mathematical. Physics*, vol. 6, pp. 1204-1209.

Power, H., Barraco, W. A. (2002): Comparison analysis between unsymmetric and symmetric RBFCMs for the numerical solution of PDEs. *Computers & Mathematics with Applications*, vol. 43, pp. 551-583.

Šarler, B., Vertnik, R. (2006): Meshfree explicit local radial basis function collocation method for diffusion problems. *Computers & Mathematics with Applications*, vol. 51, pp. 1269-1282.

Soliman, A. A. (2006): A numerical simulation and explicit solutions of KdV-Burgers' and Lax's seventh-order KdV equations. *Chaos, Solitons & Fractals*, vol. 29, pp. 294-302.

Su, C. H., Gardner, C. S. (1969): Derivation of the Kortewege–de Vries and Burgers' equation. *Journal of Mathematical Physics*, vol. 10, pp. 536-539.

Talaat, S., El-Danaf, A. (2008): Septic B-spline method of the Kortewege-de Varies-Burgers' equation. *Communications in Nonlinear Science and Numerical Simulation*, vol. 13, pp. 554-566.

Tolstykh, A. I., Shirobokov, D. A. (2003): On using radial basis functions in a "finite difference mode" with applications to elasticity problems. *Computational Mechanics*, vol. 33, pp. 68-79.

Vertnik, R., Šarler, B. (2006): Meshless local radial basis function collocation method for convective-diffusive solid-liquid phase change problems. *International Journal of Numerical Methods for Heat & Fluid Flow*, vol. 16, pp. 617-640.

Whitham, G. B. (1974): *Linear and non-linear waves*. New York: Wiley.

Wright, G. B., Fornberg, B. (2006): Scattered node compact finite difference-type formulas generated from radial basis functions. *Journal of Computational Physics*, vol. 212, pp. 99-123.

Zaki, S. I. (2000): A quintic B-spline finite elements scheme for the KdVB equation. *Computer Methods in Applied Mechanics and Engineering*, vol. 188, pp. 1211134.